nature genetics

An ENU-induced mutation of miR-96 associated with progressive hearing loss in mice

Morag A Lewis[1], Elizabeth Quint[2], Anne M Glazier[1], Helmut Fuchs[3], Martin Hrabé De Angelis[3], Cordelia Langford[1], Stijn van Dongen[1], Cei Abreu-Goodger[1], Matias Piipari[1], Nick Redshaw[4], Tamas Dalmay[4], Miguel Angel Moreno-Pelayo[5,6], Anton J Enright[1] & Karen P Steel[1,2]

Progressive hearing loss is common in the human population, but little is known about the molecular basis. We report a new *N*-ethyl-*N*-nitrosurea (ENU)-induced mouse mutant, diminuendo, with a single base change in the seed region of *Mirn96*. Heterozygotes show progressive loss of hearing and hair cell anomalies, whereas homozygotes have no cochlear responses. Most microRNAs are believed to downregulate target genes by binding to specific sites on their mRNAs, so mutation of the seed should lead to target gene upregulation. Microarray analysis revealed 96 transcripts with significantly altered expression in homozygotes; notably, *Slc26a5*, *Ocm*, *Gfi1*, *Ptprq* and *Pitpnm1* were downregulated. Hypergeometric *P*-value analysis showed that hundreds of genes were upregulated in mutants. Different genes, with target sites complementary to the mutant seed, were downregulated. This is the first microRNA found associated with deafness, and diminuendo represents a model for understanding and potentially moderating progressive hair cell degeneration in hearing loss more generally.

Progressive hearing loss is common in the human population. About one in 850 children are born with a significant, permanent hearing impairment, but by the age of ten this number has doubled[1]. Age-related hearing loss in later life has a heritability approaching 50%[2], and some single genes have been identified underlying progressive hearing loss in rare families (see URLs section below). However, for the vast majority of cases of progressive hearing loss there is no molecular diagnosis. To provide candidate genes and models for hearing loss, we established a screen for new ENU-induced deaf mouse mutants[3]. One such mutant recovered was diminuendo (*Dmdo*), inherited in a semidominant manner. Heterozygotes (*Dmdo*/+) show a progressive loss of the Preyer reflex (ear flick response to sound) between 4 and 6 weeks. Homozygotes (*Dmdo*/*Dmdo*) do not have a Preyer reflex at any age, and show head bobbing and a staggering, circling gait.

The gross structure of the middle and inner ears appeared normal in mutants, so we examined the organ of Corti using scanning electron microscopy. At 4–5 d after birth, the number and arrangement of hair cells appeared normal in mutants, and heterozygotes looked similar to wild-type littermates (**Fig. 1a** and **Supplementary Fig. 1a**,**b** online). However, irregular bundles and persistent clusters of ectopic stereocilia were observed in homozygotes (**Fig. 1b–d**), and by 7 d, homozygote hair cells showed marked degeneration (data not shown). At 4 and 6 weeks old, very few recognizable hair cells remained in homozygotes (**Supplementary Fig. 1f**,**k**). In heterozygotes, many outer hair cells had degenerated in the middle and basal turns but most inner hair cells remained intact (**Supplementary Fig. 1l–o**). Remaining outer hair cell stereocilia bundles formed a loose U shape rather than the precise V shape of controls, and inner hair cells often showed smaller, more widely separated bundles (**Fig. 1e–h** and **Supplementary Fig. 1e**,**h**,**j**,**p**,**q**). Compound action potentials, reflecting cochlear nerve activity in response to sound, were undetectable in homozygotes at 4 weeks, and in heterozygotes thresholds were raised by around 60 dB (**Supplementary Fig. 1r**), despite the persistence of many surviving hair cells. Endocochlear potentials were within the normal range (**Supplementary Fig. 1s**). Fused stereocilia and hair cell degeneration were evident in the vestibular systems of 4-week-old heterozygotes.

We mapped the mutant phenotype to proximal chromosome 6, between *D6Mit159* and *D6Mit268*, a 4.96-Mb interval (**Supplementary Fig. 2a**,**b** online). We sequenced 87% of the ~900 exons within the interval and located two mutations. The first mutation was a silent C>T substitution in exon 5 of *2310005E10Rik*, encoding a member of the aldo-keto reductase family and a putative ortholog of the human gene *AKR1B10*. The mutated base is the third in the codon, and the amino acid, asparagine, is not affected. The variant in the *Dmdo* genome is identical to the equivalent wild-type human reference sequence. Normalized cDNA from the organs of Corti of three 4-d-old (P4) *Dmdo*/*Dmdo* and +/+ sibling pairs gave bands of identical size and intensity when subjected to PCR with primers in

[1]Wellcome Trust Sanger Institute, Hinxton, UK. [2]Medical Research Council, Institute of Hearing Research, Nottingham, UK. [3]GSF National Research Center for Environment and Health, Munich, Germany. [4]School of Biological Sciences, University of East Anglia, Norwich, UK. [5]Unidad de Genética Molecular, Hospital Ramón y Cajal, Madrid, Spain. [6]Centro de Investigación Biomédica en Red de Enfermedades Raras (CIBERER), ISCIII, Madrid, Spain. Correspondence should be addressed to K.P.S. (kps@sanger.ac.uk).

Received 25 June 2008; accepted 13 February 2009; published online 12 April 2009; doi:10.1038/ng.369

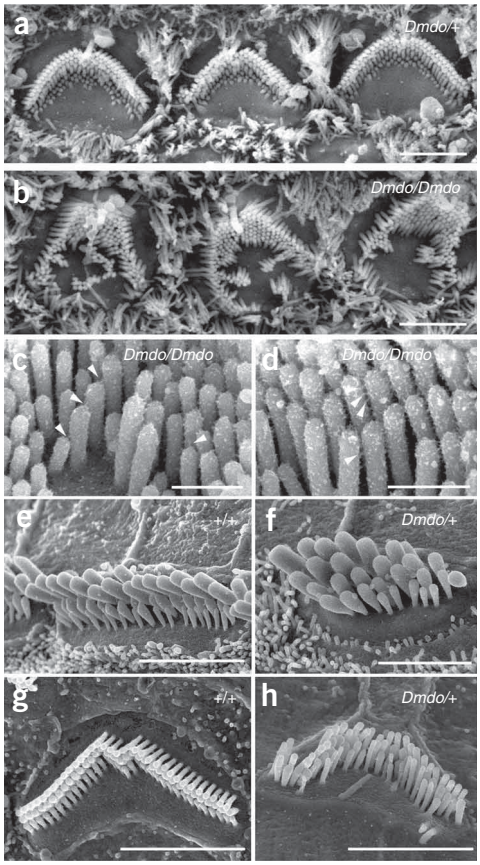

Figure 1 Scanning electron micrographs of diminuendo inner ear. (**a**,**b**) Heterozygote (**a**, *Dmdo*/+) and homozygote (**b**, *Dmdo/Dmdo*) at P5, showing irregular hair bundles and ectopic stereocilia. Scale bars, 2 μm. (**c**,**d**) Stereocilia in homozygotes at P4 showing tip links (**c**; arrowheads) and lateral links (**d**; arrowheads). Scale bars, 500 nm. (**e**–**h**) Stereocilia bundles of inner hair cells (**e**,**f**) and outer hair cells (**g**,**h**) in heterozygotes (**f**,**h**) and wild-type littermates (**e**,**g**) at P28. Scale bars, 3 μm (**e**,**g**,**h**) and 2 μm (**f**). Heterozygous outer hair cells (**h**) show irregular stereocilia bundles, have a smaller apical surface, and are more widely spaced than in wild types. Inner hair cells also appear to be more widely separated and show smaller bundles with fewer stereocilia organized in 4–5 rows (**f**). All *Dmdo*/+ stereocilia have rounded tips.

exons 4 and 6. We concluded that this variant was unlikely to be involved in causing the hearing impairment in the diminuendo mutant (**Supplementary Fig. 2c**,**d**).

The second mutation was an A>T substitution in *Mirn96* (*mmu-miR-96*; miR-96), a microRNA (miRNA). MicroRNAs are small noncoding RNAs that bind to specific sites in the 3′ UTR of target mRNAs, inducing transcript destabilization and translational inhibition. The mutation lies within the miRNA seed region (nucleotides 2–7), which confers binding specificity[4], making this variant a strong candidate for the causative mutation. The sequence of mature miR-96 is perfectly conserved between human, mouse, rat and fish (**Fig. 2a**).

Mirn96 is one of a cluster of three miRNAs; the other two are *Mirn183* and *Mirn182*. These miRNAs are expressed in all sensory hair cells of the inner ear and in neurons of the cochlear and vestibular ganglia in newborn mice, and are thought to be processed from a single primary transcript[5]. We found that all three mature miRNAs were expressed in hair cells of both wild types and homozygous mutants (**Fig. 2b**–**g**), suggesting the mutation does not have a major effect on processing and export of the miRNAs to the cytoplasm despite the possible interference of the mutation with stem loop formation required for cleavage of the transcript[6].

We chose two complementary approaches to study the effects of the mutation. First, we used the miRanda target predictor v3.0 (ref. 7) with additional filtering to produce a list of 132 genes, which we annotated (**Supplementary Table 1** online); we then selected 13 genes for further study (**Supplementary Table 2** online). We used a luciferase assay with siRNAs mimicking the wild-type and mutant miR-96. The siRNAs were co-transfected into NIH 3T3 cells with a construct containing the 3′ UTR of each candidate gene, either with the putative binding sites intact, or with the sites replaced by an *Eco*RI site to disrupt binding. Five genes were validated as targets of miR-96: *Aqp5*, *Celsr2*, *Myrip*, *Odf2* and *Ryk* (**Supplementary Fig. 3a**,**b** online). Quantitative RT-PCR showed that *Aqp5* and *Celsr2* were significantly

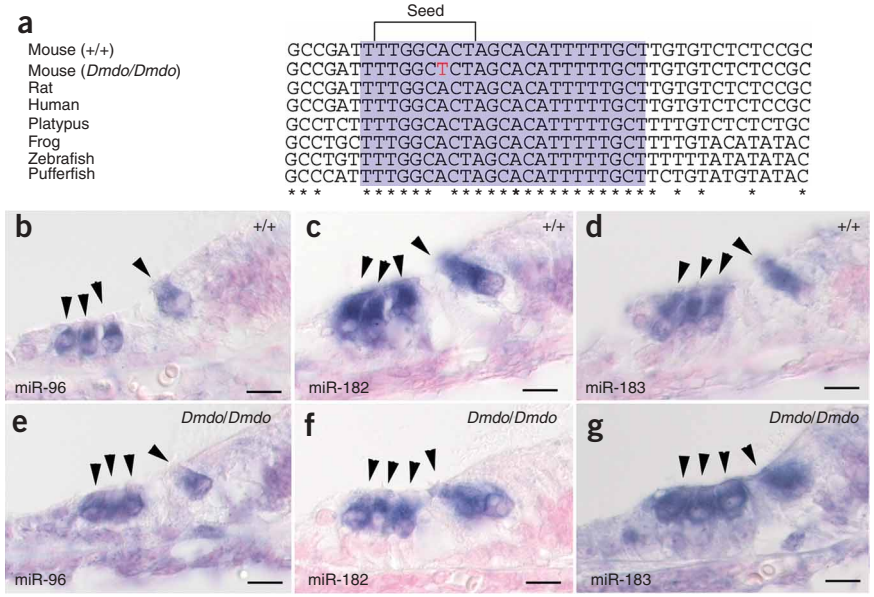

Figure 2 miR-96, miR-182 and miR-183 in littermates at P5. (**a**) Alignment of DNA sequences from wild-type mouse, diminuendo homozygote, rat, human, platypus, frog, zebrafish and pufferfish. The mature miRNA sequence for each species is shaded purple, and the seed region critical for target binding is bracketed. The mutation, indicated by the red letter, falls within the seed region. The mature sequence is absolutely conserved between the species shown, and also between cow, dog, horse, macaque, opossum, chimpanzee, orangutan, ground squirrel, tree shrew, mouse lemur, bushbaby, cat, armadillo, tenrec, medaka, rabbit, stickleback and tetraodon (sequences obtained from Ensembl v50). (**b**–**d**) Expression of miR-96 (**b**), miR-182 (**c**) and miR-183 (**d**) in wild type. (**e**–**g**) Expression of miR-96 (**e**), miR-182 (**f**) and miR-183 (**g**) in homozygotes. No specific staining was observed using the control probe (data not shown). Probes designed against the mature miRNA sequence have been shown incapable of detecting the precursor transcript[29], so these show the location of only the mature miRNA. Hair cells are marked by arrowheads. Scale bars, 10 μm.

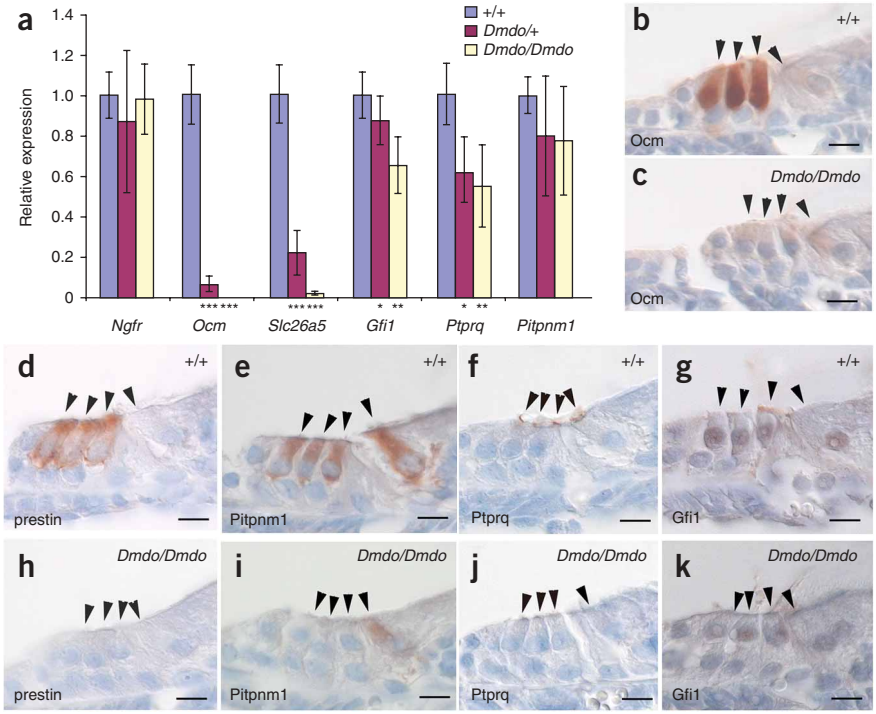

Figure 3 *Ocm*, *Slc26a5*, *Pitpnm1*, *Ptpr1* and *Gfi1* expression in diminuendo. (**a**) Quantitative real-time PCR on cDNA generated from normalized RNA from the organs of Corti of 4-d-old littermates. *Ocm*, *Slc26a5*, *Ptprq* and *Gfi1* are downregulated in heterozygotes and homozygotes. Error bars, s.d. Quantities normalized to *Hprt1* levels; *Ngfr* is expressed in support cells adjacent to hair cells[30] and was used to assess the quantity of sensory material. *Ngfr*: wild type, $n = 12$, mean = 1.01 ± 0.12 (s.d.); heterozygote, $n = 12$, mean = 0.89 ± 0.35 (s.d.); homozygote, $n = 12$, mean = 0.99 ± 0.17 (s.d.). *Ocm*: wild type, $n = 9$, mean = 1.01 ± 0.15 (s.d.); heterozygote, $n = 9$, mean = 0.07 ± 0.04 (s.d.); homozygote, $n = 9$, mean = 0.003 ± 0.001 (s.d.). *Slc26a5*: wild type, $n = 9$, mean = 1.01 ± 0.14 (s.d.); heterozygote, $n = 9$, mean = 0.22 ± 0.11 (s.d.); homozygote, $n = 9$, mean = 0.02 ± 0.01 (s.d.). *Gfi1*: wild type, $n = 9$, mean = 1.01 ± 0.12 (s.d.); heterozygote, $n = 9$, mean = 0.88 ± 0.12 (s.d.); homozygote, $n = 9$, mean = 0.66 ± 0.14 (s.d.). *Ptprq*: wild type, $n = 9$, mean = 1.01 ± 0.15 (s.d.); heterozygote, $n = 9$, mean = 0.62 ± 0.18 (s.d.); homozygote, $n = 9$, mean = 0.56 ± 0.20 (s.d.). *Pitpnm1*: wild type $n = 8$, mean = 1.00 ± 0.09 (s.d.); heterozygote, $n = 9$, mean = 0.80 ± 0.29 (s.d.); homozygote, $n = 9$, mean = 0.78 ± 0.27 (s.d.). Three animals were used for each genotype and DNA from each was run in triplicate. *t*-tests: *Ngfr* heterozygote $P = 0.25$ (Welch's *t*-test), homozygote $P = 0.75$ (Student's *t*-test); *Ocm* heterozygote $P = 1.51 \times 10^{-8}$ (Welch's *t*-test), homozygote $P = 3.46 \times 10^{-8}$ (Welch's *t*-test); *Slc26a5* heterozygote $P = 7.73 \times 10^{-10}$ (Student's *t*-test), homozygote $P = 3.37 \times 10^{-8}$ (Welch's *t*-test); *Gfi1* heterozygote $P = 0.038$ (Student's *t*-test), homozygote $P = 3.39 \times 10^{-5}$ (Student's *t*-test); *Ptprq* heterozygote $P = 1.37 \times 10^{-4}$ (Student's *t*-test), homozygote $P = 6.46 \times 10^{-5}$ (Student's *t*-test); *Pitpnm1* heterozygote $P = 0.084$ (Welch's *t*-test), homozygote $P = 0.35$ (Student's *t*-test); $\alpha = 0.05$. $^{***}P < 1 \times 10^{-7}$. $^{**}P < 1 \times 10^{-4}$. $^{*}P < 0.05$. (**b**–**k**) Location of oncomodulin (**b**,**c**), prestin (**d**,**h**), Pitpnm1 (**e**,**i**), Ptprq (**f**,**j**) and Gfi1 (**g**,**k**) in 5-d-old wild-type (**b**,**d**–**g**) and homozygote (**c**,**h**–**k**) littermates. Scale bars, 10 μm.

upregulated in mutant cochlear tissues compared with wild type (*Aqp5*: $P = 0.013$, Welch's *t*-test; *Celsr2*: $P = 0.00278$, Student's *t*-test). However, the difference in expression was small (**Supplementary Fig. 3c**). We used antibodies against the validated targets and found that all five were expressed in or near wild-type hair cells at P3 and P5, but there was no visible difference in diminuendo (**Supplementary Fig. 3d–m** and data not shown). However, miRNAs may have multiple small effects on the expression of a number of genes[8] and immunohistochemical tests may not show such small effects. Therefore, we adopted a genome-wide approach to investigate the mechanism of action of the mutation.

We compared gene expression of both direct and indirect targets by microarray analysis of the organ of Corti of P4 mutants and wild types. We retrieved 96 significantly affected transcripts ($P < 0.05$); 50 genes were upregulated and 36 downregulated (**Supplementary Table 3** online); the remaining 10 probes were either duplicates (6) or mapped to intergenic regions (4). Thirteen of these so far have been confirmed by qRT-PCR (**Supplementary Fig. 4a** online). Of the downregulated genes, five in particular were of interest: *Slc26a5* (prestin), *Ocm* (oncomodulin), *Pitpnm1*, *Gfi1* and *Ptprq*. None of these genes has a predicted wild-type or mutant miR-96 target site, so the downregulation is presumably a downstream effect. Prestin is a voltage-sensitive motor molecule that mediates outer hair cell length changes responsible for amplification of sound within the cochlea[9]. Prestin knockout mice have short hair cells and hair cell degeneration[10]. Oncomodulin is expressed in outer hair cells and may act as a cytosolic calcium ion buffer[11]. Ptprq is required for maturation of the hair bundle, and is thought to be a component of interstereocilial shaft connectors[12]. *Gfi1* is expressed in hair cells, and knockout mice show hair cell degeneration[13]. The difference in expression of these genes was confirmed by qRT-PCR in both heterozygotes and homozygotes (**Fig. 3a**) and by immunohistochemistry (**Fig. 3b–k**). We did not find any evidence of genomic changes that might account for the extreme downregulation of *Ocm* and *Slc26a5*: exon 1 of each gene amplified correctly in mutants, surrounding genes were expressed normally in the microarray, and the diminuendo phenotype showed mendelian inheritance and mapped to the *Mirn96* locus. Epigenetic downregulation of any one of these five genes could explain the hearing impairment, as three are known to lead to deafness when knocked out and the remaining two are highly expressed in sensory hair cells.

We asked whether the striking downregulation of oncomodulin and prestin was a generic feature of degenerating hair cells by looking at immunostaining intensity in nine other mouse mutants that show early hair cell degeneration: headbanger and shaker1^{4626SB} (*Myo7a*)[14,15], Snell's waltzer (*Myo6*)[16], headturner (*Jag1*)[17], beethoven and deafness (*Tmc1*)[18,19], oblivion (*Atp2b2*)[20], catweasel (*Six1*)[21] and whirler (*Whrn*)[22]. Oncomodulin and prestin showed hair cell labeling in mutants as strong as in the littermate controls (**Supplementary Fig. 5a–p** online and data not shown), suggesting that the reduction of expression in diminuendo was a specific feature. Furthermore, other markers of hair cells and supporting cells of the organ of Corti showed normal immunostaining intensity in diminuendo mutants at P0, P3 and P5, including *Myo7a*, *Cdkn1b* (*p27*^{Kip1}), *Sox2* and *Jag1* (**Supplementary Fig. 5q–y** and data not shown).

We next searched for wider miRNA effects on the mRNA profile of diminuendo using Sylamer[23]. Analysis of all miRNA heptamers shows

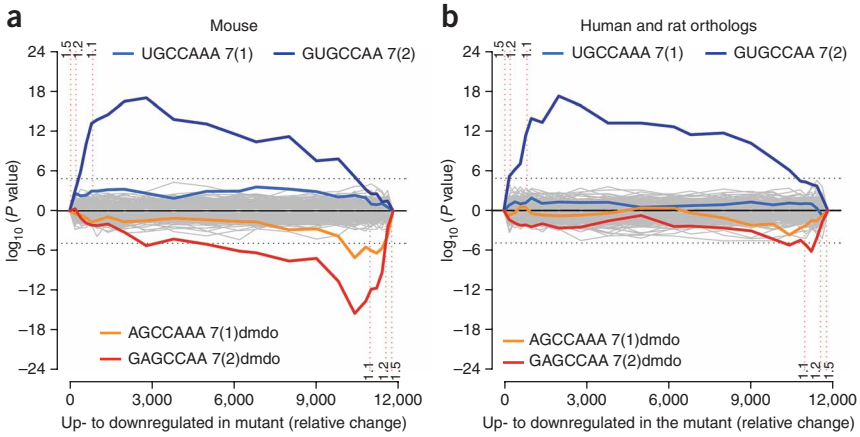

Figure 4 Microarray analysis showing enrichment and depletion of heptamers in 3′ UTRs. (**a**) Microarray analysis showing enrichment and depletion of heptamers in 3′ UTRs using Sylamer[23]. The *x* axis represents the sorted gene list from most upregulated (left) to most downregulated (right). The *y* axis shows the hypergeometric significance for enrichment or depletion of heptamers in 3′ UTRs at leading parts of the gene list. Positive values indicate enrichment ($-\log_{10}(P)$) and negative values depletion ($\log_{10}(P)$). Heptamers that are depleted in the initial part are accordingly enriched in the complementary part with the same *P* value, as a consequence of the hypergeometric distribution. For each miRNA (including the diminuendo mutant miR-96), the two heptamers matching the 5′ seed region, starting at positions 1 and 2, were considered. Each heptamer was tested at regularly placed rank cutoffs in the gene list. The *P* value indicates the significance of the enrichment or depletion of the heptamer in the set of 3′ UTRs in the initial part of the gene list when compared to the 3′ UTRs in the complementary set. The horizontal dotted lines represent an E-value threshold (*P* value corrected for multiple testing) of 0.01. Vertical dotted lines indicate fold change cutoffs of >1.5, >1.2 and >1.1, and the parts of the gene lists defined by these cutoffs. (**b**) The same analysis as in **a**, where each 3′ UTR has been replaced by the concatenation of its orthologous 3′ UTRs in human and rat. The seed match for the wild-type miR-96 shows similar enrichment as compared with the analysis in **a**. In contrast, the enrichment of the miR-96 diminuendo mutant binding sites in the downregulated genes is barely above background (dotted line).

that the heptamer complementary to the seed region of miR-96 (GUGCCAA) is greatly enriched in the 3′ UTRs of hundreds of genes upregulated in diminuendo homozygotes (**Fig. 4**). This indicates that miR-96 normally modulates expression of a broad range of target genes, and that it affects mRNA levels rather than translation alone. Among the most downregulated genes, the heptamer complementary to the mutant miR-96 is enriched (GAGCCAA; **Fig. 4**), indicating that mutant miR-96 influences expression of newly acquired target genes. We analyzed conservation of these signals. Wild-type seed matches are enriched in 3′ UTRs of human and rat orthologs of the most upregulated mouse genes (**Fig. 4**), suggesting that these sites are conserved and may be functional. However, enrichment of mutant miR-96 binding sites in human and rat orthologs of downregulated genes is barely above significance threshold (dotted line). We also used a simple log ratio analysis of seed match biases in gene sets at different cutoffs (**Supplementary Fig. 4b–j**); these results agreed with the Sylamer analysis.

To elucidate the link between the mutated microRNA and the abnormally expressed genes revealed by the microarray analysis, we examined the 500 bp upstream of the top 356 upregulated genes and the top 425 downregulated genes to find any transcription factor motifs that were enriched in the affected genes (**Supplementary Fig. 4k–n**). Several interesting motifs were found, including a *Gfi1*-like motif found among the upregulated genes; a binding site for Mitf, known to be regulated by miR-96 (ref. 24); and targets associated with control of Notch signaling, such as Pou2f1 (ref. 25), Rbpj[26] and bHLH transcription factors[27]. Any one of the transcription factor binding motifs discovered could be involved in linking the mutation in miR-96 to the misregulation of genes directly required for hair cell development and survival. The large number of genes whose expression is affected by miR-96 and the complexity of their interactions suggest that there may not be a simple mechanism that explains the effects of the mutation, but rather a combination of many small effects that act in concert to cause hair cell dysfunction.

The diminuendo mutant shows progressive hearing impairment in heterozygotes and profound deafness in homozygotes associated with hair cell defects. Although hearing impairment is often thought to be caused by hair cell loss, this and previous studies suggest that the degeneration is instead a correlate or consequence of a prior dysfunction of the hair cells. The mutation in the seed region of miR-96 is highly likely to cause the hearing impairment in diminuendo mutants because it cosegregates with the phenotype, it occurs in the seed region of the miRNA known to be critical for target recognition, miR-96 is expressed specifically in the cells most affected by the mutation, Sylamer analysis indicated that the mutation has a direct effect on expression of many genes as well as indirect effects, and we found no other plausible mutation despite resequencing the vast majority of the coding sequence within the nonrecombinant region of chromosome 6. In addition, the finding of two different single base changes in the seed region of miR-96 in humans with progressive hearing loss in an accompanying report[28] provides critical support for our proposal that the single base change in miR-96 is the causative mutation behind the diminuendo phenotype, and furthermore suggests that the phenotype results from a lack of repression of normal targets even though we show a gain of repression of newly identified targets. Although the link between the direct targets of the miRNA and the phenotype are not clear, we have shown that several genes known to be important for hair cell function are specifically downregulated in the diminuendo mutant and any one could account for the hair cell dysfunction. This is the first ENU-induced mutation found in an miRNA and the first miRNA found to be associated with deafness. Understanding the mechanism by which miR-96 leads to progressive hearing loss will give us clues to help develop therapies to ameliorate the effects of progressive deafness, whatever the trigger.

METHODS

Phenotyping, genetic mapping and mutation screening. We recovered the diminuendo mutant from a screen for new dominantly inherited mutations using *N*-ethyl-*N*-nitrosurea (ENU) as a mutagen. Electron microscopy was carried out on inner ears of mice at 4 and 5 d old, and 4 and 6 weeks old, using the OTOTO method. We recorded compound action potentials and endocochlear potentials using standard techniques. The mutation was localized using a backcross and genome scan, followed by sequencing of the exons within the nonrecombinant region. Additional details are provided in **Supplementary Methods**, **Supplementary Table 4** and **Supplementary Note** online.

RNA extraction. The organs of Corti of 4-d-old mice were dissected and stored at −20 °C in RNAlater stabilization reagent (QIAgen, cat. no. 76106). We

extracted RNA using QIAshredder columns (QIAgen, cat. no. 79654) and the RNeasy mini kit (QIAgen, cat. no. 74104), following the manufacturer's instructions.

Expression analysis. Pups were collected on the day they were born, or 3 or 5 d after birth. Animals were dissected in ice-cold PBS, fixed for two days in 10% formalin at 4 °C, embedded in paraffin and cut into 8-µm sections. We carried out immunohistochemistry and *in situ* hybridizations using the Ventana Discovery machines and reagents according to the manufacturer's instructions. From each animal, at least five sections were used per probe or antibody. Quantitative RT-PCR was carried out on cDNA from normalized organ of Corti RNA, using reagents from Applied Biosystems.

Transfections and luciferase assays. A region of the 3′ UTR of each candidate gene containing the putative target site(s) for miR-96 was amplified and inserted into a luciferase-containing plasmid. Details of the regions of the 3′ UTRs of each candidate gene may be found in **Supplementary Table 5** online.

URLs. Hereditary hearing loss homepage, http://webh01.ua.ac.be/hhh/.

Accession codes. ArrayExpress: the microarray data has been deposited under accession number E-TABM-489.

Note: Supplementary information is available on the Nature Genetics website.

ACKNOWLEDGMENTS

We thank P. Ellis, K. James and R. Andrews for assistance with the microarrays, H. Williams for help with the quantitative RT-PCR, A. Rodriguez for helpful discussions on miRNAs, A. Taylor for help with bioinformatics, S. Rose, M. Drummond, K. Hawker and A. Lucas for help with mapping the mutation, F. Zhu for her work on Gfi1 and Ptprq, R. Lacey and D. Savage for animal care, A. El-Amraoui and C. Petit for the anti-MyRIP antibody, G. Richardson for the anti-Ptprq antibody, and A. Rzadzinska for high-resolution scanning electron microscopy analysis. This work was supported by Deafness Research UK, the Wellcome Trust, Medical Research Council (UK), EC (CT-97-2715, LSHG-CT-2004-512063), Spanish Ministerio de Ciencia y Tecnología (SAF2005-06355), Spanish Fondo de Investigaciones Sanitarias (FIS PI-051942; G03/203, CP03/00014, PI08/0045), NGFN (Germany), and charitable donations from individuals affected by deafness.

AUTHOR CONTRIBUTIONS

The mutagenesis programme was carried out by H.F. and M.H.D.A.; E.Q. analyzed the behavior, the middle and inner ear and the ultrastructural phenotype of the mutant and mapped the mutation. M.A.L., E.Q. and A.M.G. sequenced the region. Microarrays were run by C.L., and bioinformatic analysis was carried out by S.v.D., C.A.-G. and A.J.E. Motif analysis was done by M.P.; N.R. and T.D. carried out the luciferase assays. Literature searches, *in situ* hybridization, immunohistochemistry, quantitative RT-PCR and data analyses were done by M.A.L.; M.A.M.-P. shared data and ideas. K.P.S. conceived and devised the screen for new deaf mutants, obtained the funding, managed the programme, carried out the electrophysiology and interpreted the data. The paper was written by M.A.L., E.Q. and K.P.S.

Published online at http://www.nature.com/naturegenetics/
Reprints and permissions information is available online at http://npg.nature.com/reprintsandpermissions/

1. Fortnum, H.M., Summerfield, A.Q., Marshall, D.H., Davis, A.C. & Bamford, J.M. Prevalence of permanent childhood hearing impairment in the United Kingdom and implications for universal neonatal hearing screening: questionnaire based ascertainment study. *Br. Med. J.* **323**, 536–540 (2001).
2. Gates, G.A., Couropmitree, N.N. & Myers, R.H. Genetic associations in age-related hearing thresholds. *Arch. Otolaryngol. Head Neck Surg.* **125**, 654–659 (1999).
3. Hrabe de Angelis, M. *et al.* Genome-wide, large-scale production of mutant mice by ENU mutagenesis. *Nat. Genet.* **25**, 444–447 (2000).
4. Lewis, B.P., Burge, C.B. & Bartel, D.P. Conserved seed pairing, often flanked by adenosines, indicates that thousands of human genes are microRNA targets. *Cell* **120**, 15–20 (2005).
5. Weston, M.D., Pierce, M.L., Rocha-Sanchez, S., Beisel, K.W. & Soukup, G.A. MicroRNA gene expression in the mouse inner ear. *Brain Res.* **1111**, 95–104 (2006).
6. Duan, R., Pak, C. & Jin, P. Single nucleotide polymorphism associated with mature miR-125a alters the processing of pri-miRNA. *Hum. Mol. Genet.* **16**, 1124–1131 (2007).
7. Enright, A.J. *et al.* MicroRNA targets in *Drosophila*. *Genome Biol.* **5**, R1 (2003).
8. Shivdasani, R.A. MicroRNAs: regulators of gene expression and cell differentiation. *Blood* **108**, 3646–3653 (2006).
9. Dallos, P. *et al.* Prestin-based outer hair cell motility is necessary for mammalian cochlear amplification. *Neuron* **58**, 333–339 (2008).
10. Liberman, M.C. *et al.* Prestin is required for electromotility of the outer hair cell and for the cochlear amplifier. *Nature* **419**, 300–304 (2002).
11. Sakaguchi, N., Henzl, M.T., Thalmann, I., Thalmann, R. & Schulte, B.A. Oncomodulin is expressed exclusively by outer hair cells in the organ of Corti. *J. Histochem. Cytochem.* **46**, 29–39 (1998).
12. Goodyear, R.J. *et al.* A receptor-like inositol lipid phosphatase is required for the maturation of developing cochlear hair bundles. *J. Neurosci.* **23**, 9208–9219 (2003).
13. Wallis, D. *et al.* The zinc finger transcription factor Gfi1, implicated in lymphomagenesis, is required for inner ear hair cell differentiation and survival. *Development* **130**, 221–232 (2003).
14. Holme, R.H. & Steel, K.P. Stereocilia defects in waltzer (*Cdh23*), shaker1 (*Myo7a*) and double waltzer/shaker1 mutant mice. *Hear. Res.* **169**, 13–23 (2002).
15. Rhodes, C.R. *et al.* A *Myo7a* mutation cosegregates with stereocilia defects and low-frequency hearing impairment. *Mamm. Genome* **15**, 686–697 (2004).
16. Self, T. *et al.* Role of myosin VI in the differentiation of cochlear hair cells. *Dev. Biol.* **214**, 331–341 (1999).
17. Kiernan, A.E. *et al.* The Notch ligand *Jagged1* is required for inner ear sensory development. *Proc. Natl. Acad. Sci. USA* **98**, 3873–3878 (2001).
18. Bock, G.R. & Steel, K.P. Inner ear pathology in the deafness mutant mouse. *Acta Otolaryngol. (Stockh.)* **96**, 39–47 (1983).
19. Vreugde, S. *et al.* Beethoven, a mouse model for dominant, progressive hearing loss DFNA36. *Nat. Genet.* **30**, 257–258 (2002).
20. Spiden, S.L. *et al.* The novel mouse mutation Oblivion inactivates the PMCA2 pump and causes progressive hearing loss. *PLoS Genet.* **4**, e1000238 (2008).
21. Bosman, E.A., Quint, E., Fuchs, H., de Angelis, M.H. & Steel, K.P. Catweasel mice: a novel role for *Six1* in sensory patch development and a model for Branchio-Oto-Renal syndrome. *Dev. Biol.* advance online publication, doi:10.1016/j.ydbio.2009.01.030 (2 February 2009).
22. Mburu, P. *et al.* Defects in whirlin, a PDZ domain molecule involved in stereocilia elongation, cause deafness in the whirler mouse and families with DFNB31. *Nat. Genet.* **34**, 421–428 (2003).
23. van Dongen, S., Abreu-Goodger, C. & Enright, A.J. Fast assessment of microRNA binding and siRNA off-target effects from expression data. *Nat. Methods* **5**, 1023–1025 (2008).
24. Xu, S., Witmer, P.D., Lumayag, S., Kovacs, B. & Valle, D. MicroRNA (miRNA) transcriptome of mouse retina and identification of a sensory organ-specific miRNA cluster. *J. Biol. Chem.* **282**, 25053–25066 (2007).
25. Kiyota, T., Kato, A., Altmann, C.R. & Kato, Y. The POU homeobox protein Oct-1 regulates radial glia formation downstream of Notch signaling. *Dev. Biol.* **315**, 579–592 (2008).
26. Kato, H. *et al.* Functional conservation of mouse Notch receptor family members. *FEBS Lett.* **395**, 221–224 (1996).
27. Kageyama, R. & Ohtsuka, T. The Notch-Hes pathway in mammalian neural development. *Cell Res.* **9**, 179–188 (1999).
28. Mencia, A. *et al.* Mutations in the seed region of the human miR-96 are responsible for nonsyndromic progressive hearing loss. *Nat. Genet.* advance online publication, doi:10.1038/ng.355 (12 April 2009).
29. Obernosterer, G., Leuschner, P.J.F. & Alenius, M. Post-transcriptional regulation of microRNA expression. *RNA* **12**, 1161–1167 (2006).
30. Mueller, K.L., Jacques, B.E. & Kelley, M.W. Fibroblast growth factor signaling regulates pillar cell development in the organ of Corti. *J. Neurosci.* **22**, 9368–9377 (2002).